The Role of Microbubble Dose in Combined Microflotation of Fine Particles

Nickolaj Rulyov *

Posted Date: 26 December 2023

doi: 10.20944/preprints202312.1909.v1

Keywords: fine particles; microbubbles; combined microflotation, particle transfer

Article

The Role of Microbubble Dose in Combined Microflotation of Fine Particles

Nickolaj Rulyov

Institute of Biocolloid Chemistry, National Academy of Sciences of Ukraine, Head of the Department of Physico-Chemical Hydrodynamic of Ultra-disperse Systems 42 Vernadsky av., 03142 Kyiv, UKRAINE; nrulyov@gmail.com; Tel.: +380-50-311-5846

Abstract: Flotation of small particles is one of the global challenges facing the mineral raw materials processing industry. Large amounts of non-ferrous and rare metals are lost in the flotation tailings in the form of mineral particles below 15 μm in size as a result of the low effectiveness of their capture by coarse bubbles generated in conventional flotation machines. The method of combined microflotation, which has been developed in recent years, uses not only coarse but also microbubbles (MB) produced in the stand-alone generator of air-in-water microdispersion, which serves as the flotation carriers. Depending on the dose of MB, the effect of their application may be both positive and negative. The theoretical analysis of various mechanisms of particle transfer onto the surface of coarse bubbles and further into the froth layer allowed to obtain the formula for the optimal MB dose $f = 2\,d_d/d_p\rho_p$, **where** d_d **is MB size;** d_p **and** ρ_p **respectively are the size and the density of particles**. Experiments performed on the copper ore flotation tailings at the Atalaya Mining (Spain) and Chaarat Kapan (Armenia) concentrators showed that, besides the optimal MB dose in the range of 1-3 ml/g, there is another optimal MB dose in the range of 10-20 ml/g, where the copper recovery increases by several percent compared to the reference test ($f = 0$). In the area between the optimal MB doses, the deep minimum in copper recovery is observed, which value is by several percent lower compared to the value in the reference test.

Keywords: fine particles; microbubbles; combined microflotation; particle transfer

1. Introduction

Flotation presents one of the major and commonly applied methods for the beneficiation of non-ferrous and rare metal ores. Unfortunately, this method is not sufficiently effective for small particle flotation because of the losses of considerable amounts of valuable metals in the form of fine ore particles smaller than 15 μm into tailings. With the depletion of rich deposits and a noticeable shift to developing poor finely disseminated ores, the challenge of fine particle flotation assumes greater importance [1]. It is already well established, theoretically [2–5], as well as experimentally [6–9], that the flotation rate is fundamentally dependent on the efficiency of particle capture by a rising bubble and, in the first approximation, proportional to the value d_p^2/D_B^2, where d_p and D_B are particles and bubbles sizes respectively. Thus, it follows that the efficient flotation of particles smaller than 15 μm requires the application of bubbles smaller than 200 μm. Unfortunately, the bubbles produced in most conventional flotation cells are coarser, approximately by the order of magnitude [10]. Several methods of small generating have been developed and are available [11], yet their implementation in the industry is accompanied by serious issues. In particular, the method discussed in [12,13] involves pulp saturation with microbubbles by passing the pulp through the electrolyzer with insoluble electrodes. And though the laboratory tests provided sufficiently positive results of the flotation of fine particles smaller than 15 μm, implementation of this method in practice raises concerns because of the formation of large amounts of oxygen and hydrogen gas mixture. Currently, two types of flotation machines are used, in which relatively small microbubbles (MB) are generated by the method of dispersing air and the cavitation effect due to the impact of a pulp jet on the water/air interface (Jameson Cell) [14] or alternatively through the collision with an obstruction inside the pulp, as well as passing the pulp and air mixture through venturi tubes (IMHOFLOT Cell) [15].

Preprints (www.preprints.org) | NOT PEER-REVIEWED | Posted: 26 December 2023 doi:10.20944/preprints202312.1909.v1

Unfortunately, the mentioned methods would not ensure the generation of sufficient quantities of bubbles less than 100 μm in size, which is critical for the flotation of ultrafine mineral particles.

It has already been established [16] that in conventional mechanical flotation machines, the process of flotation by coarse bubbles could be enhanced by applying a relatively small number of fine bubbles, which in this case will essentially be as flotation carriers. A theoretical explanation for this effect was given in [17]. This mode of fine particle flotation is now termed combined microflotation (CMF), as it is based on the use of fine and coarse bubbles.

The high effectiveness of the CMF of ultrafine particles has been proven by multiple laboratory tests with artificial and natural mineral mixtures [18–20]. In all test runs, microbubbles were generated by mechanically dispersing air in a frother solution. Depending on the concentration and activity of the frother, the air-in-water microdispersion thus produced contained up to 60 vol. % microbubbles of the dimensions in the range 10 to 100 μm. The dispersion obtained by this mode could be directed through a pipe to any spot in the flotation chamber where the most intense mixing occurs.

It was initially assumed that the greater the dose of MB per unit mass of floated particles is, the more pronounced the effect of flotation enhancement should be. However, further theoretical and experimental findings have demonstrated that the optimal dose of MB is significantly dependent on the density and size of particles, and if the dosage of MB is not set correctly, the application of MB may have a negative impact on the flotation process.

The purpose of this study is to define how the dosage of MB affects the effectiveness of CMF and also establish critical factors that influence this optimal dosage value.

2. Theory

2.1. Mechanisms of particle transfer into the froth layer

Figure 1 shows graphic layouts for various mechanisms of particle transfer onto the surface of a coarse bubble (CB) and into the froth layer.

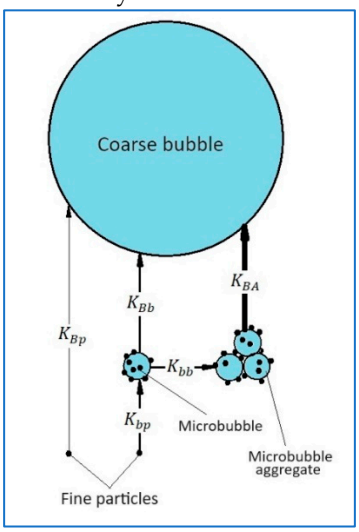

Figure 1. Pattern of various mechanisms of transfer of particles onto the surface of a coarse bubble.

Mechanism I comprises the direct deposition of a particle on the surface of a rising CB under the effects of surface and hydrodynamic forces. The rate constant of this process is determined by the relation [7]

$$K_{Bp} = \frac{3qE}{2D_B} \quad (1)$$

where q is the superficial air velocity induced by CB flow, D_B is their diameter, E denotes the capture efficiency of a particle by bubbles that is determined by the ratio [6]

Preprints (www.preprints.org) | NOT PEER-REVIEWED | Posted: 26 December 2023 doi:10.20944/preprints202312.1909.v1

$$E = \frac{3d_p^2}{2D_B^2}\alpha_{Bp} \tag{2}$$

where d_p is particle size, α_{Bp} is the coefficient which reflects the effects of surface and hydrodynamic forces involved in the interaction of a particle with the surface of a bubble. Thus, from formulas (1) and (2) it follows that

$$K_{Bp} = \frac{3qd_p^2}{2D_B^3}\alpha_{Bp} \tag{3}$$

Mechanism II of the particle transfer to the CB surface comprises the sequence of two events: first is the deposition of a particle on the surface of an MB, and second is the attachment of MB on the CB surface. Since the sedimentation of both MB and small particles occurs very slowly, the settlement of particles on the MB surface will mostly occur due to the non-uniformity of the hydrodynamic field in a flotation cell. In this case, the rate constant of the process can be estimated by the formula [21]

$$K_{bp} = \frac{4G\varphi_b}{3\pi}\varepsilon(d_p/d_b) \tag{4}$$

where d_b is the diameter of the SB, G is the average shear rate of the medium, φ_b is the volume concentration of MB in pulp, $\varepsilon(d_p/d_b)$ is the probability of a particle attachment to the surface of the bubble when they collide in a simple shear field. As it was previously shown [22], in the case where $d_p \ll d_b$, the function $\varepsilon(d_p/d_b)$ takes the form

$$\varepsilon = \frac{d_p^2}{d_b^2}\gamma \tag{5}$$

where γ is the parameter dependent on the nature of the surface forces of interaction between the particle and the MB. From formulas (4) and (5) it follows that the rate constant of the first stage is

$$K_{bp} = \frac{4G\varphi_b d_p^2}{3\pi d_b^2}\gamma \tag{6}$$

When it comes to the second stage, then by the analogy with the above process of direct deposition of particles on CB surface, we obtain the ratio for the rate constant shown below

$$K_{Bb} = \frac{3qd_b^2}{2D_B^3}\alpha_{Bb} \tag{7}$$

where α_{Bb} is the probability of MB attachment on the CB surface under the action of the surface forces. As the rate of the chain of successive events equals the rate of the slowest one, the rate of the second mechanism of particle deposition onto CB is determined by the smaller of the two rate constants K_{bp} and K_{Bb}.

Mechanism III of the particle transfer to CB comprises the sequence of three events: 1 presents the deposition of a particle on the MB surface; 2 involves combining MB into aggregates, and 3 is actually the deposition of MB aggregates on the surface of the CB or alternatively directly into the froth layer. According to the Smoluchowski equation modified with the account of aggregates porosity [23], which describes the process of particles aggregation in the simple shear field, we obtain

$$\frac{d[d_A(t)]}{dt} = \frac{4G\varphi_b\lambda}{3\pi(1-p)}d_A(t) \tag{8}$$

where d_A is the dimension of MB aggregates; p is their porosity; λ is the probability of MB to-form an aggregate at their collision in the simple shear flow. This probability depends on the ratio of the surface and hydrodynamic forces. Hence the rate constant of the second stage can be estimated by the formula

Preprints (www.preprints.org) | NOT PEER-REVIEWED | Posted: 26 December 2023 doi:10.20944/preprints202312.1909.v1

$$K_{bb} = \frac{4G\varphi_b\lambda}{3\pi(1-p)} \quad (9)$$

In terms of the third stage, then by the analogy with the immediate deposition of MB on the CB, the process rate constant can be expressed as

$$K_{BA} = \frac{3qd_A^2}{2D_B^3}\alpha_{BA} \quad (10)$$

where α_{BA} is the probability of MB aggregates to deposit on CB's surface, which is determined by the ratio of the surface and hydrodynamic forces. In brief, the rate of mechanism III shall be determined by the smallest of the rate constants K_{bp}, K_{bb} and K_{BA}. Since either of the parameters γ, λ, α_{Bp}, α_{Bb}, α_{BA} is smaller than unity, hence in formulas (3, 6, 7, 9 and 10) we assume these parameters as equal to unity, and this will allow us to estimate the maximum values of the rate constants of sub-processes involved in the particle transfer into the froth layer. For illustration purposes, Table 1 shows the particle transfer rate constants for the above three mechanisms, which are calculated for the most probable parameters of the flotation process. Presented data show that the rates of particle transfer into the froth layer vary depending on the mechanism, and the rate of mechanism II is by an order of magnitude, and mechanism III is by two orders of magnitude faster compared to that by mechanism I, and the particle deposition onto MB occurs practically instantly. The value d_A = 0.1 mm is selected on the reason that it is close to the size limit of particle floatability [24]. At the same time, we should consider that very large aggregates loaded with light particles (for example, coal or quartz particles) can be independently entrained into the froth layer, as observed in [18,20].

Table 1. Rate constants of particle transfer sub-processes for particle concentration 0.3 g/L.

Maximal Subprocess Rate constant min^{-1}	Mechanism I	Mechanism II	Mechanism III
K_{Bp}	0.01		
K_{bp}		34	34
K_{Bb}		0.1	
K_{bb}			11
K_{BA}			1.1
$K_{minimal}$	0.01	0.1	1.1

Parameters
d_p = 0.01 mm
ρ_p = 4.3 g/cm^3
d_b = 0.03 mm
d_A = 0.1 mm
f_{opt} = 1.4 mL/g
$\varphi_{b\,opt}$ = 4.2·10^{-4}
D_B = 2 mm
G = 3.6·10^4 min^{-1}
q = 600 mm/min
p = 0.4

2.2. Optimal microbubble dosage

The essential precondition for the functioning of the third, most effective mechanism of particle transfer onto the CB surface is the formation of aggregates from MB loaded with particles. Since hydrophobic particles act like bridges, which, similarly to flocculants, bind MB into aggregates, it is necessary that the volumetric dose of MB per unit weight of floated particles is optimal. If the MB dose is very low, then their surface will be practically completely occupied by particles, and hence, they cannot form aggregates. But if the MB dose is quite high, there could be too few particles, so the probability of aggregate formation due to bridges of hydrophobic particles could be very low. Consequently, there must be some optimal dose of MB, which is dependent on the size and on the density of particles, as well as on the size of the MB.

The practice of using flocculants shows [25], that the optimal MB dose should be set so as to ensure the coverage of half of the MB surface by particles. Let's assume that the number concentration of MB in the pulp is n_b, and the number of floated particles is n_p. Then the volumetric dose of SB per the unit weight of particles f can be expressed by the formula

Preprints (www.preprints.org) | NOT PEER-REVIEWED | Posted: 26 December 2023 doi:10.20944/preprints202312.1909.v1

$$f = \frac{n_b d_b^3}{n_p d_p^3 \rho_p} \tag{11}$$

где ρ_p is the particles density. The share of MB surface that could be taken by particles can be estimated using the formula

$$k_s = \frac{n_p d_p^2}{n_b d_b^2} \tag{12}$$

where k_s is the coefficient of MB surface coverage. Combining the formulas (11) and (12), we arrive at

$$f = \frac{d_b}{d_p \rho_p k_s} \tag{13}$$

Assuming that in (13) $k_s = 1/2$, we obtain the expression for the optimal MB dose

$$f_{opt} = \frac{2 d_b}{d_p \rho_p} \tag{14}$$

As it follows from the formula (14), the optimal dosage of MB increases with the decrease of particle dimension and their density. Thus, for example, the optimal MB dose for quartz will be four times higher than that for particles of chalcocite of the same dimensions.

Obviously, particle transfer mechanisms onto CB shall depend on the MB dosage. For illustration purposes, Figure 2a shows the diagram for the case when the small bubble dose is significantly below the optimal one. In this case, all small bubbles will be completely covered by particles very fast, and the particles will block the aggregation, and the transfer of particles on CB will occur mostly by mechanism I. In the opposite case, shown in Figure 2b, where the MB dose is slightly below the optimal, the greater share of particles will attach to the bubble surface, thus blocking the aggregation, and the particle transfer will occur mostly by mechanism II. If the MB dose is optimal, then as shown in Figure 2c, small bubbles can form aggregates, and the particle transfer will happen primarily by mechanism III. Finally, if the MB dose is significantly higher than the optimal, then as it is shown in Figure 2d, the coverage of their surface will be minor, and the probability of their aggregation or attachment onto the CB surface will be low.

Of course, at some doses of MF, the transfer of particles onto the CB can occur simultaneously by two or three of the mentioned mechanisms. Besides, in the flotation of light particles, so large aggregates can form that they can rise into the frother layer without assistance from CB. As an example, Figure 3 shows.

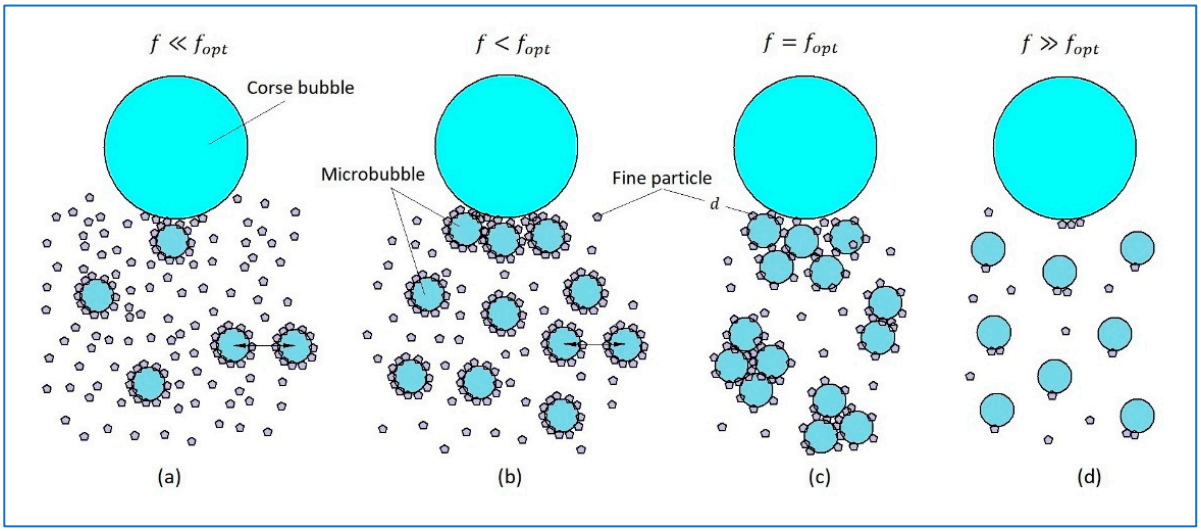

Preprints (www.preprints.org) | NOT PEER-REVIEWED | Posted: 26 December 2023 doi:10.20944/preprints202312.1909.v1

Figure 2. The diagram of particle transfer on CB surface at various MB doses.

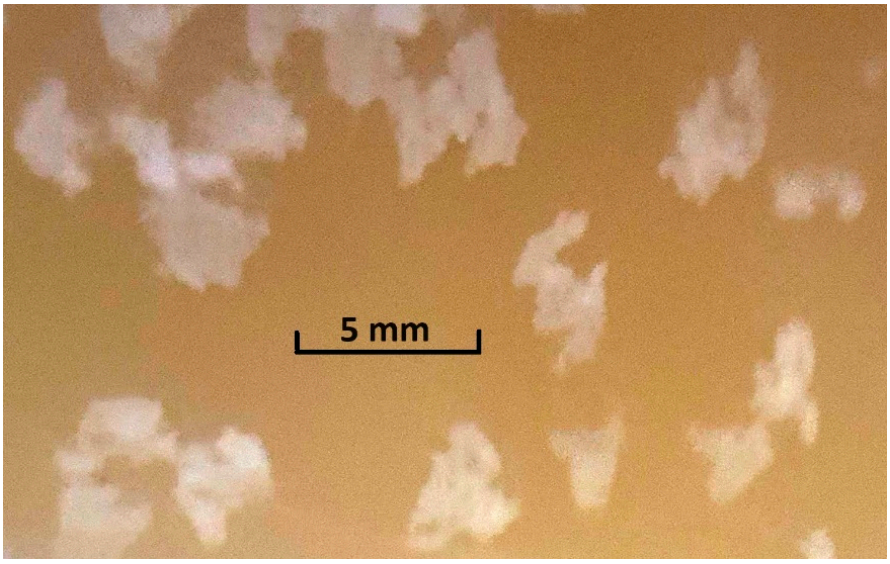

Figure 3. Aggregates formed of MB and glass beads on the pulp surface.

3. Experimental

For the purposes of validating the above-mentioned theoretical considerations, a series of laboratory studies were conducted, including the tests of the effectiveness of CMF on the copper ore tailings at the concentrators ATALAYA MINING (Spain) and CHAARAT KAPAN (Armenia). In these tests, the air-in-water microdispersion was produced and fed into the flotation cell by the MBGen-0.012 generator provided by TURBOFLOTSERVICE Company (Ukraine), shown in Figure 4 below. This unit has the capacity to generate up to 12 L/h of microdispersion, containing up to 58 vol.% of microbubbles of 10-100 μm in size. Therefore, the required dosage of SM could be fed into the cell in 5-15 s.

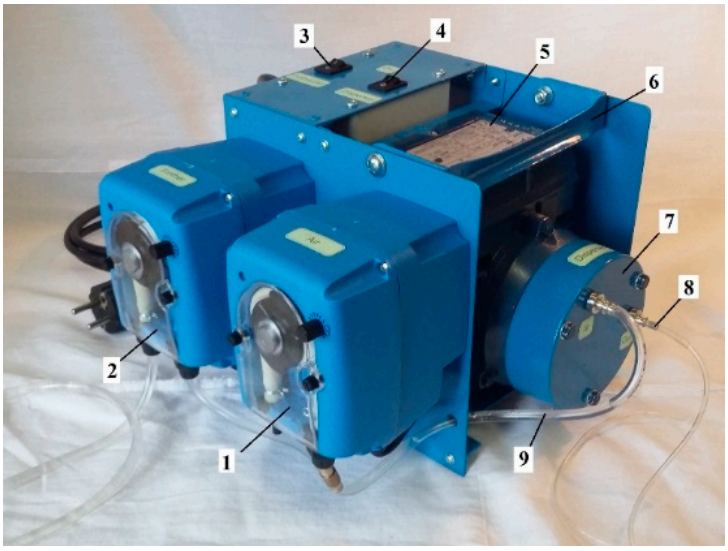

Figure 4. MBGen-0.012 generator of air-in-water microdispersion:.1, 2 -peristaltic dosing pumps of air and frother solution, respectively; 3-push buttons for feeding air and frother solution; 4-start button of dispergator driver; 5- dispergator driver; 6- the handle; 7- dispergator head; 8-outlet pipe for air-in-water microdispersion; 9- inlet pipe for feeding air-in-water mixture into the dispergator head.

3.1. Atalaya Mining

Preprints (www.preprints.org) | NOT PEER-REVIEWED | Posted: 26 December 2023 doi:10.20944/preprints202312.1909.v1

Flotation tests were conducted in a 2.7 L laboratory cell with the automatic collection of froth concentrate in 5-second froth scraping intervals. The test run specifications are: total flotation time - 10 min; impeller speed - 900 rpm; airflow rate - 3 L/min. The frother used in the tests were DOWFROTH 250 and OREPREP F549. The solids concentration in the pulp varied in the range of 327 – 423 g/L; the copper content in the feed was in the range of 0.064 – 0.078 %; the chalcopyrite concentration in the pulp was 0.21-0.33 g/L; frother concentration in pulp was 5.1 mg/L. The introduction of microbubbles in the flotation cell was arranged via a narrow silicon tube before the start of flotation.

As shown in Figure 5 and 6, copper recovery dependencies on the MB dose per one mass unit of chalcopyrite reach the extreme pattern with maximums at low and high doses. As the optimum dose f_{opt}, as it follows from the graphs, is about 1.75 mL/g, then substituting this value in the formula (14), and the value for the chalcopyrite density ρ_p = 4.3, we obtain d_b/d_p = 3.8. The presence of a sufficiently deep minimum between the two maxima of copper recovery values can be explained by the fact that when the MB dose is getting much higher than the optimal one, the process of formation of large aggregates accelerates, and the aggregates become are so large that, as mentioned above, they cannot be retained on the CB any longer, yet they are not coarse enough to overcome the convective flows inside the flotation cell independently and rise into the frother layer. As Figure 4 shows, a further increase in MB dose promotes the formation of aggregates that are so large themselves that they start to rise like CB, and, in fact, this factor explains the presence of a sufficiently high maximum in the recovery in the MB dose range that is by order of magnitude higher than the optimal one f_{opt}. Finally, the decrease in recovery after the second maximum can be attributed to the fact that at gigantic MB doses, the number of particles on them decreases so much that the probability of MB aggregates formation, or MB attachment onto the CB, drops practically to zero.

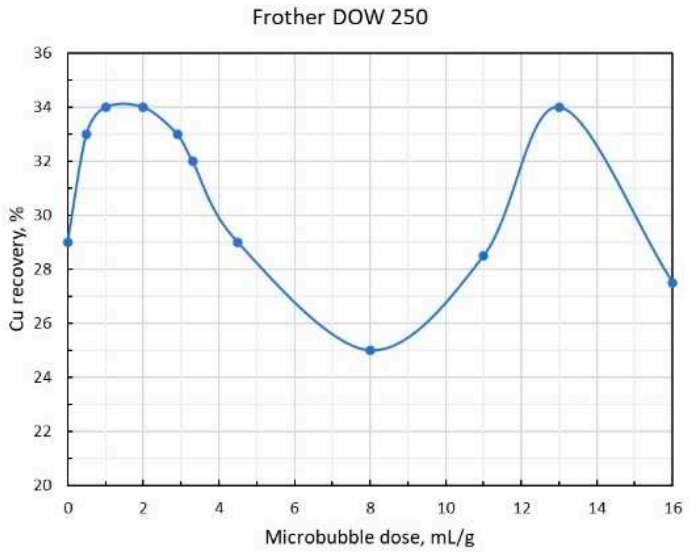

Figure 5. Dependence of copper recovery on MB dose per mass unit of chalcopyrite: The solid concentration in pulp is 357- 423 g/L; the copper content in the feed is 0.067-0.078 %; chalcopyrite concentration is 0.24 - 0.33 g/L; the Frother DOWFROTH 250.

Preprints (www.preprints.org) | NOT PEER-REVIEWED | Posted: 26 December 2023 doi:10.20944/preprints202312.1909.v1

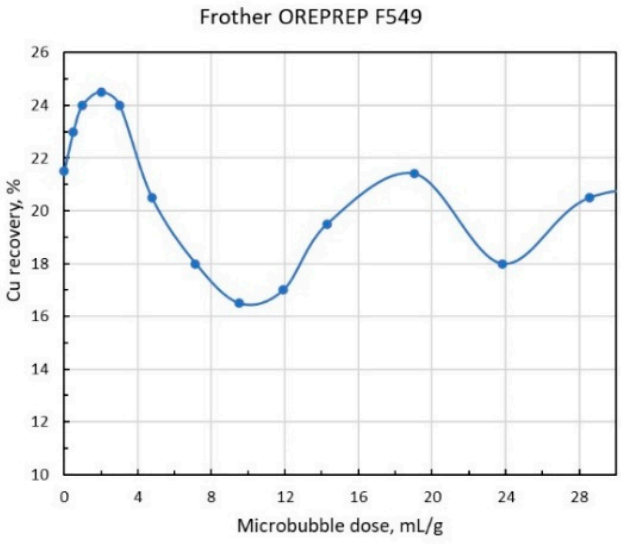

Figure 6. Dependence of copper recovery on MB dose per mass unit of chalcopyrite: Solid concentration in pulp is 326 - 383 g/L; copper content in the feed is 0.064-0.072 %; chalcopyrite concentration is 0.21 - 0.28 g/L; Frother OREPREP F549.

3.2. Chaarat Kapan

Rougher copper tailings (i.e., copper scavenger feed) flotation tests were conducted in a 2.7 L laboratory flotation cell for 10 minutes at an impeller speed of approx. 900 rpm and airflow rate 0.12 L/min. Flomin F-650 frother was used in all tests for MB production in the MBGen-0.012 generator. The solids concentration in the pulp was 234-247 g/L; the copper content in the form of chalcopyrite particles was 0.086-0.094%; the chalcopyrite concentration in the pulp was 0.20-0.3 g/L; frother concentration in pulp was 3.1 mg/L. The introduction of microbubbles in the flotation cell was arranged via a narrow silicon tube before the start of flotation.

Figure 7 shows the dependence of copper recovery on SB dose. In this test, two maxima were observed in the range of small and large SB doses, while when the doses increased above 12 mL/g, a significant blocking in chalcopyrite flotation occurred.

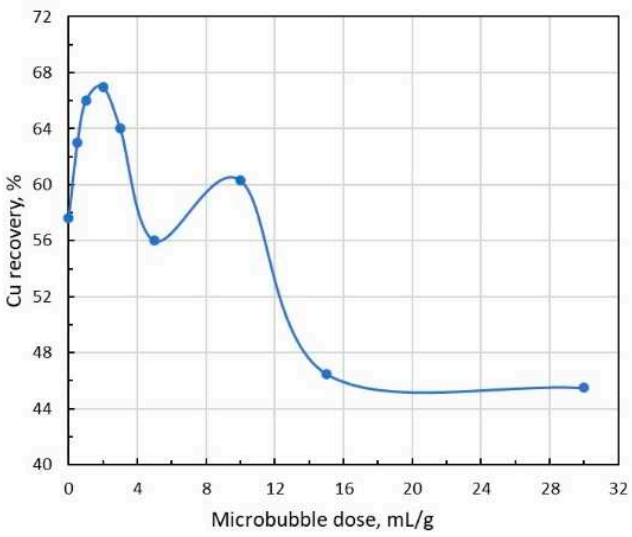

Figure 7. The dependence of copper recovery from tailings of the Cu-scavenging flotation stage on the MB dose per mass unit of chalcopyrite: The solids concentration in the pulp was 234-247 g/L; the copper content in the form of chalcopyrite particles was 0.086-0.094%; the chalcopyrite concentration in the pulp was 0.20-0.32 g/L.

4. Conclusions

1. Combined microflotation of small particles involves three main mechanisms for particles transfer onto the coarse bubble surface and their further transport into the frother layer: 1-direct deposition of particles onto the surface of coarse bubbles; 2- deposition of particles onto the surface of microbubbles, which in their turn deposit on coarse bubbles; 3- deposition of particles onto the surface of microbubbles that combine into aggregates, and the aggregates, in their turn, deposit on coarse bubbles or independently rise into the froth layer.
2. There are two doses of microbubbles for the ranges of their small and large values.
3. In the range of small values, the optimal dose of microbubbles can be estimated by the formula $f_{opt} = \frac{2d_b}{d_p\rho_p}$, where d_b is the microbubbles dimension, d_p and ρ_p are the particles size and density respectively.

Funding: This research received external funding from TMR Technology Inc.

Data Availability Statement: The data presented in this study are available on request from the corresponding author. The data are not publicly available due to the privacy of the patients who assisted in the research.

Acknowledgments: The author expresses his thanks and appreciation to TMR Technology Inc. in the person of President Alken Kuanbay for the arrangements and financing of the tests at the Atalaya Mining (Spain) and Chaarat Kapan (Armenia) concentrators and also wishes to thank the employees of these companies for their technical assistance in the test runs and chemical examination of flotation products. Special thanks to the TURBOFLOTSERVICE company (Ukraine, Kyiv) that provided the MBGen-0.012 air-in-water microdispersion generator.

Conflicts of Interest: The author declares no conflict of interest.

Abbreviations

MB Microbubble
CB Coarse bubble
CMF Combined microflotation

References

1. Farrokhpay, S.; Filippov, L; Fornasiero, D. Flotation of Fine Particles: A Review. *Mineral Processing and Extractive Metallurgy Review* **2020**, DOI: https://10.1080/08827508.2020.1793140
2. Sutherland, K.L. Physical Chemistry of Flotation. XI. Kinetics of the Flotation Process. *The Journal of Physical and Colloid Chemistry* **1948**, 52, 394-425.
3. Gaudin, A.M. *Flotation*, 2nd ed.; McGraw-Hill: New York, 1957.
4. Anfruns, J.F.; Kitchener, J.A. The rate of capture of small particles in flotation. *Trans. Instit. Mining Metall. Section C* **1977**, 86, C9.
5. Derjaguin, B.V.; Dukhin, S.S.; Rulev, N.N. Kinetic theory of flotation of small particles. *Surface and Colloid Science*; Plenum Press: N.Y. - London, 1984; pp. 71-113.
6. Tomlinson, H.S.; Fleming, M.G. Flotation Rate Studies. *Mineral Processing: 6-th International Congress* (Cannes, June 1963): Pergamon Press, London: 1965, pp. 562-573.
7. Flint, L.R.; Howarth, W.J. Collision efficiency of small particles with spherical air bubbles. *Chem. Eng. Sci.* **1971**, 26, 1155-1168.
8. Reay, D.; Ratcliff, G. A. Removal of fine particles from water by dispersed air flotation- effects of bubble size and particle size on collection efficiency. *Canadian Journal of Chemical Engineering* **1973**, 53, 178-185.
9. Reay, D.; Ratcliff, G. A. Effects of Bubble Size and Particle Size of Collection Efficiency. *Canadian Journal of Chemical Engineering* **1975**, 53, 481-486.
10. Sawyerr, F.; Deglon, D.A.; O'Connor, C.T. Prediction of bubble size distribution in mechanical flotation cells. *The Journal of The South African Institute of Mining and Metallurgy* **1998**, July/August, 179-185.
11. Jung, M.U.; Kim, Y.C.; Bournival, G.; Ata, S. Industrial application of microbubble generation methods for recovering fine particles through froth flotation: A review of the state-of-the-art and perspectives. *Advances in Colloid and Interface Science* **2023**, 103047, https://doi.org/10.1016/j.cis.2023.103047.
12. Glembotsky, V.A.; Mamakov, A.A.; Romanov, A.M.; Nenno, V.E. Selective separation of fine mineral slimes using method of electric flotation. In *Proceedings of 11th International Mineral Processing Congress*, Cagliari, 1975, pp. 561-582.

13. Bhaskar Raju, G.; Khangaonkar, P. R. Electro-flotation of chalcopyrite fines. *International Journal of Mineral Processing* **1982**, 9, 133–143.
14. Harbort, G.; De Bono, S.; Carr, D.; Lawson, V. Jameson Cell fundamentals – a revised perspective. Minerals Engineering **2003**, 16(11), 1091-1101. http://dx.doi.org/10.1016/j.mineng.2003.06.008
15. Imhof, R.; Fletcher, M.; Vathavooran, A.; Singh, A. Application of Imhoflot G-Cell centrifugal flotation technology. The journal of The Southern African Institute of Mining and Metallurgy **2007**, 107, 623-631.
16. Glembotsky, V.A.; Klassen, V.I. *Flotation*, Nedra, Moskau, 1973.
17. Rulyov, N.N. Combined microflotation of fine minerals: Theory and Experiment, *Mineral Processing and Extractive Metallurgy (Trans. Inst. Min. Metall. C)* **2016**, 125, Issue 2, 81-85.
18. Rulyov, N.N.; Filippov, L.O.; Kravchenko, O.V. Combined Microflotation of Glass Beads. *Colloids and Surfaces A: Physicochemical and Engineering Aspects* **2020**, 598, 5 August, 124810 https://doi.org/10.1016/j.colsurfa.2020.124810
19. Rulyov, N.N.; Filippov, L.O.; Sadovskyi, D.Y.; Lukianova, V.V. Reverse combined microflotation of fine magnetite from the mixture with glass beads. *Minerals* **2020**, 10, 0; https://doi:10.3390/min10110000
20. Rulyov, N.; Sadovskiy, D.; Rulyova, N.; Filippov, L. Column flotation of fine glass beads enhanced by their prior heteroaggregation with microbubbles. *Colloids and Surfaces A: Physicochemical and Engineering Aspects* **2021**, *617* 126398. https://doi.org/10.1016/j.colsurfa.2021.126398
21. Van de Ven, T.G.M.; Masson, S.G. The microrheology of colloidal dispersions. VII. Orthokinetic doublet formation of spheres. *Colloid Polym. Sci.* **1977**, 255, 468–479.
22. Adler, P.M. Heterocoagulation in shear flow. *J. Colloid Interface Sci.* 1981, 83. 106–115.
23. Rulyov, N.N.; Dontsova, T.A.; Nebesnova, T.V. The pair binding energy of particles and size flocs, which are formed in the turbulent flow. *Khimiya i Tekhnologtya Vody* **2005**, 27, 1-17.
24. Ralston, J.; Fornasiero, D.; Grano, S.; Duan, J.; AkroydInt, T. Reducing uncertainty in mineral flotation-flotation rate constant prediction for particles in an operating plant ore. *J. Miner. Process* **2007**, 84, 89-98.
25. Gregory, J. Polymer adsorption and flocculation in sheared suspensions. *Colloids & Surface* **1988**, 31:231245.